Optim Eng
DOI 10.1007/s11081-009-9092-4

Fuzzy genetic optimization on performance-based seismic design of reinforced concrete bridge piers with single-column type

Yu-Chi Sung · Chin-Kuo Su

Received: 16 December 2008 / Accepted: 10 August 2009

Abstract This paper presents a fuzzy genetic optimization for performance-based seismic design (PBSD) of reinforced concrete (RC) bridge piers with single-column type. The design is modeled as a constrained optimization problem with the objective of minimizing construction cost subject to the constraints of qualified structural capacity and suitable reinforcement arrangements for the designed RC pier. A violation of the constraints is combined with construction cost to serve as the objective function. The fuzzy logic control (FLC), which adapts the penalty coefficients in the genetic algorithm (GA) optimization solver, was employed to avoid a penalty that is too strong or too weak through the entire calculation so that a feasible solution can be obtained efficiently.

The reported results of cyclic loading tests for three piers with square section, rectangular section and circular section, respectively, were employed as the data-base of investigation. Furthermore, a case study on the PBSD of a square RC bridge pier with four required performance objectives (fully operational, operational, life safety and near collapse) corresponding to different peak ground accelerations (PGAs) of earthquakes was analyzed. Six feasible designs of the pier were determined successfully and the optimal one with minimum construction cost was obtained accordingly. The result obtained shows that the proposed algorithm gives an acceptable design for the PBSD of the RC bridge piers.

The superiorities of GA and FLC were incorporated and the availability of the proposed procedure was investigated. Moreover, through the proposed systematic design procedure, the discrepancy in the PBSD from different design engineers will be lessened effectively and the design efficiency as well as the design precision will also be enhanced significantly.

Y.-C. Sung (✉) · C.-K. Su
Department of Civil Engineering, National Taipei University of Technology, Taipei 106, Taiwan
e-mail: sungyc@ntut.edu.tw

C.-K. Su
e-mail: s3679002@ntut.edu.tw

Published online: 27 August 2009

Keywords Minimum construction cost · Penalty coefficient · Pushover analysis · Structural performance

1 Introduction

The performance-based seismic design (PBSD) of a reinforced concrete (RC) bridge pier with single-column type intends to find a feasible design consistent with multiple-level structural performances with respect to different levels of earthquake. Its primary goal is to determine the nonlinear performance of structures under different scales of severe earthquakes for safety or retrofitting considerations, or the linear performance of structures under moderate earthquakes for detecting their serviceability or operational functions (SEAOC 1995; ATC-40 1996). In other words, the complete structural performance excited from moderate earthquakes up to the maximum loading, which may lead to ultimate states, is required for design. Making a qualified design that satisfies the rigorous limitations is difficult even for the senior engineers, and an indirect investigation procedure is widely adopted as an alternative. A set of design parameters for an RC pier including the material strengths, the arrangement of reinforcements and the size of pier section is able to be tried initially, based on the designer's experience. Certain important characteristics such as plastic hinge property (PHP) and sensitivity to structural nonlinearity of the pier can be determined accordingly (Sung et al. 2005). Sequentially, the seismic response of the single-column pier is able to be evaluated rapidly via a pushover analysis if a simple model of the cantilever structure is considered. If the response obtained does not meet the target of structural performance, the design parameters need to be revised and the process needs to be repeated until the targeted structural performance is satisfied. A highly iterative trial-and-error design procedure is often used and the accuracy as well as the efficiency of the design is strongly sensitive to the designer's experience. Therefore, the goal of this work is to create a systematic design procedure to avoid the man-made discrepancy and enhance the design precision.

In this paper, the PBSD of an RC bridge pier was modeled as a constrained optimization problem with the objective of minimizing construction cost subject to the constraints of qualified structural capacity and suitable reinforcement arrangements for the designed RC pier. The structural capacity, represented by the structural force-displacement relation, obtained from the pushover analysis is required to satisfy the extreme case of multiple-level structural performances with respect to various earthquakes; the reinforcement arrangements is limited to the specification of the seismic design code of RC structure (ACI Committee 318x 2005). A violation of the constraints is combined with construction cost to serve as the objective function. Since the objective function is not able to be formulated in an explicit mathematical function, conventional optimization solvers (such as the sequential quadratic method or the dual method) are not suitable for this problem (Bazaraa and Shetty 1979).

Based on the Darwin's survival-of-the-fittest, the GA does the optimization with a group of chromosomes known as a population. Since a population provides a list of solutions at the same time, it gives a stronger search than traditional optimizers by skipping the local optimal points. For the constrained optimization problem, the penalty function is employed by penalizing the infeasible solutions by reducing their fitness values in proportion to their degrees of constraint violation. Although the GA can give potential solutions, the efficiency as well as the precision of the solutions is sensitive to the penalty coefficients. The infeasible solutions with high original fitness values may remain in subsequent generations in the case where the penalty coefficient is too small, which results in the search moving toward false peaks in the infeasible region. On the contrary, the feasible solutions with low original fitness values will have no chance to retain their good characteristics in subsequent generations in the case where the penalty coefficient is too large, which yields premature convergence resulting in poor solutions. If a constant coefficient is adopted through the entire calculation, an improper penalty during different generations may be inevitable and, accordingly, give imprecise results (Sarma and Adeli 2000).

Nanakorn and Messomklin (2001) proposed an adaptive penalty function in the GA for structural design optimization. The main idea of their scheme is to fix the chance to be selected to the matting pool of the best infeasible members throughout all generations. The parameter was set as the ratio between the fitness value of the best infeasible members and the fitness value of the feasible average members. Accordingly, a modified bilinear scaling technique was employed for fitness scaling. In this way the penalty is always adjusted so that the desired degree of penalty is achieved in all generations.

Fuzzy logic control (FLC) can deal with vagueness and impreciseness in knowledge representation by the theory of fuzzy set and it is suited modeling real-world design problems that are difficult to represent in precise mathematical forms (Zadeh 1965). The FLC can handle the decision-making problem with imprecise data and provides valuable information in deciding the predominant parameters in the model. As a result, the use of FLC to adapt the penalty coefficients in the GA is appropriate.

Soh and Yang (1996) proposed a fuzzy-controlled genetic-based search for structural shape optimization. In their model, each constraint of the shape optimization problem was represented by fuzzy set theory. By introducing a fuzzy knowledge-based system (FKBS), the applicability of coupling a fuzzy rule-based system to a GA to enhance the GA search efficiency and improve its decision-making performance was illustrated.

Some successful cases of the integration of GA with FLC on structural engineering were found (Harp et al. 2009; Pourzeynali et al. 2007; Kelesoglu 2007), however, its application on seismic design seems not so much. The present paper aims at using the FLC to control the penalty of the constraints in the GA used as the optimizer for the PBSD of the RC bridge piers with single-column type. The envelopes of the reported experimental hysteresis loops of three piers were simplified to a bilinear form of the structural force-displacement relation and served as the design target. Based on the proposed procedure, several feasible solutions of pier design were determined and their structural capacities were compared with the envelopes of the experimental loops to validate the accuracy of the proposed fuzzy genetic optimization. Furthermore, a case study on the PBSD of a square RC bridge pier with four required performance objectives (fully operational, operational, life safety and near collapse) corresponding to earthquakes with peak ground accelerations (PGAs) of 0.12 g, 0.18 g, 0.30 g and 0.40 g was analyzed. Six feasible designs of the pier were determined successfully and the optimal one with minimum construction cost was obtained accordingly.

2 Optimal model for performance-based seismic design (PDSD) of the RC bridge piers with single-column type

Two groups of cross-section commonly used for the RC bridge piers were taken into account in the present paper. For the rectangular (or square) section as shown in Fig. 1a, ten design parameters are used as the design variables. They include: (1) the length of the long side h (mm); (2) the length of the short side b (mm); (3) the number of longitudinal reinforcements along the long side n_L; (4) the number of longitudinal reinforcements along the short side n_S; (5) the diameter of the longitudinal reinforcement D_L (mm); (6) the diameter of the transverse reinforcement D_T (mm); (7) the spacing of the transverse reinforcement m (mm); (8) the strength of the concrete f_c' (MPa); (9) the strength of the longitudinal reinforcement f_y (MPa) and (10) the strength of the transverse reinforcement f_{yh} (MPa). The ten parameters are represented by a design variable vector **x** for the optimization design of RC columns with rectangular (or square) section.

For the circular section as shown in Fig. 1b, eight design parameters are used as the design variables. They include: (1) the dimension of diameter D (mm); (2) the number of the longitudinal reinforcements n; (3) the diameter of the longitudinal reinforcement D_L (mm); (4) the diameter of the transverse reinforcement D_T (mm); (5) the spacing of the transverse reinforcement m (mm); (6) the strength of the concrete f_c' (MPa); (7) the strength of the longitudinal reinforcement f_y (MPa) and (8) the strength of the transverse reinforcement f_{yh} (MPa). The eight parameters are represented by a design variable vector **x** for the optimization design of RC columns with circular section.

The construction cost ψ of a designed RC bridge pier can be expressed as:

$$\psi = V_C C_C + C_S(W_{SL} + W_{ST}) \tag{1}$$

where, V_C is the volume of concrete in the designed pier, C_C is the construction cost per volume of concrete, W_{SL} and W_{ST} are the weights of the designed longitudinal re-

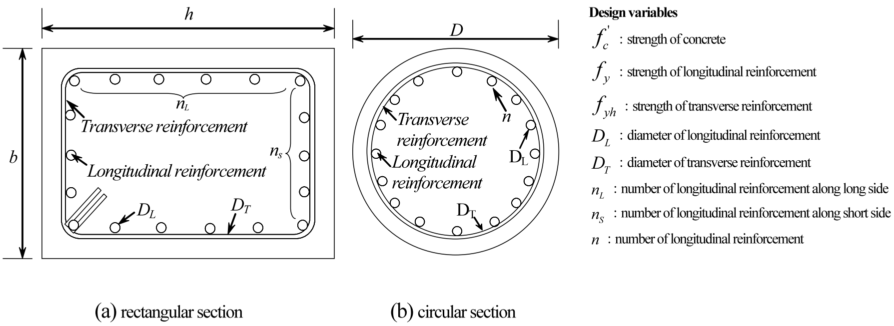

Fig. 1 Popular cross-section of reinforced concrete pier

inforcements and transverse reinforcements, respectively, and C_S is the construction cost per weight of reinforcement.

The design target (DT) of structural performance for a bridge pier is ideally modeled with a structural bi-linear system characterized by the four physical quantities which include the yielding displacement δ_Y (i.e. DT_1), the yielding force P_Y (i.e. DT_2), the ultimate displacement δ_U (i.e. DT_3), and the ultimate force P_U (i.e. DT_4). In other words, the design objectives for the target pier can be represented by (DT_i, $i = 1$–4).

On the other hand, the four design quantities (DQ): δ_Y^* (i.e. DQ_1), P_Y^* (i.e. DQ_2), δ_U^* (i.e. DQ_3) and P_U^* (i.e. DQ_4), have similar physical meanings to the design targets, and can be obtained through the pushover analysis, based on a set of design variables. Therefore, the penalties ω_i can be expressed as

$$\omega_i = \frac{|DQ_i - DT_i|}{DT_i}, \quad i = 1{-}4 \tag{2}$$

The optimization problem which seeks to minimize the function F_0 can be expressed as

$$\text{Minimize} \quad F_0(\mathbf{x}) = \psi \left(1 + \sum_{i=1}^{4} \omega_i\right)^2 \tag{3}$$

where, the square of the bracket was used to enhance the penalty for violation of the constraints (Zou and Chan 2005).

Based on the seismic design code for a RC structure (ACI Committee 318x 2005), the ratio of the cross-sectional area of the longitudinal reinforcement to the gross cross-sectional area of the RC section is defined as ρ and ρ must be between 0.01 and 0.06. The violation of the design code can be quantified by a coefficient η defined as follows

$$\eta = \begin{cases} 0 & \text{if } 0.01 \le \rho \le 0.06 \\ (\rho - 0.06)/0.06 & \text{if } \rho > 0.06 \\ (0.01 - \rho)/0.01 & \text{if } \rho < 0.01. \end{cases} \tag{4}$$

Moreover, based on ACI 318-05, the cross-sectional area A_{sh} (rectangular section) or the volumetric ratio ρ_s (circular section) of transverse reinforcement should satisfy the following equations

$$A_{sh} \ge \begin{cases} 0.09(sh_c \frac{f_c'}{f_{yh}}) \\ 0.3(sh_c \frac{f_c'}{f_{yh}})(\frac{A_g}{A_c} - 1) \end{cases} \quad \text{for rectangular section} \tag{5a}$$

$$\rho_s \ge \begin{cases} 0.12 \frac{f_c'}{f_{yh}} \\ 0.45(\frac{A_g}{A_c} - 1)\frac{f_c'}{f_{yh}}; \quad f_{yh} \le 420\ \text{MPa} \end{cases} \quad \text{for circular section} \tag{5b}$$

where h_c is the cross-sectional dimension of the column core measured center to center of confining reinforcement; A_g is the gross cross-sectional area of the column; A_c is the cross-sectional area of the column core measured out to out of transverse reinforcement; s is the spacing of transverse reinforcement that must be smaller than 10 cm and a quarter of the effective depth ($d/4$) of the column.

The violation of the design code with respect to A_{sh} (rectangular section) or ρ_s (circular section) can be quantified by a coefficient ξ as follows

$$\xi = \max \begin{cases} 0 & \text{if } A_{sh} \geq 0.09(sh_c \frac{f_c'}{f_{yh}}) \\ 0 & \text{if } A_{sh} \geq 0.3(sh_c \frac{f_c'}{f_{yh}})(\frac{A_g}{A_{ch}} - 1) \\ (0.09(sh_c \frac{f_c'}{f_{yh}}) - A_{sh})/0.09(sh_c \frac{f_c'}{f_{yh}}) & \text{if } A_{sh} < 0.09(sh_c \frac{f_c'}{f_{yh}}) \\ (0.3(sh_c \frac{f_c'}{f_{yh}})(\frac{A_g}{A_{ch}} - 1) - A_{sh}) & \\ \quad /0.3(sh_c \frac{f_c'}{f_{yh}})(\frac{A_g}{A_{ch}} - 1) & \text{if } A_{sh} < 0.3(sh_c \frac{f_c'}{f_{yh}})(\frac{A_g}{A_{ch}} - 1) \end{cases}$$

$$\text{for rectangular section} \tag{6a}$$

$$\xi = \max \begin{cases} 0 & \text{if } \rho_s \geq 0.12 \frac{f_c'}{f_{yh}} \\ 0 & \text{if } \rho_s \geq 0.45(\frac{A_g}{A_c} - 1)\frac{f_c'}{f_y} \\ (0.12 \frac{f_c'}{f_{yh}} - \rho_s)/0.12 \frac{f_c'}{f_{yh}} & \text{if } \rho_s < 0.12 \frac{f_c'}{f_{yh}} \\ (0.45(\frac{A_g}{A_c} - 1)\frac{f_c'}{f_y} - \rho_s)/0.45(\frac{A_g}{A_c} - 1)\frac{f_c'}{f_y} & \text{if } \rho_s < 0.45(\frac{A_g}{A_c} - 1)\frac{f_c'}{f_y} \end{cases}$$

$$\text{for circular section} \tag{6b}$$

The normalized coefficients η and ξ defined in (4) and (6) quantify the degree of violation of the longitudinal and transverse reinforcement, respectively, and are adopted as the input variables to the FLC which finds a scale factor $FLC(\eta, \xi)$ of the penalty coefficient λ in the GA. The details of $FLC(\eta, \xi)$ are discussed in the next section.

The constrained optimization model can be regarded as an extension of (3) and expressed as

$$\text{minimize} \quad F(\mathbf{x}) = \psi \left[1 + \sum_{i=1}^{4} \omega_i + \lambda \cdot FLC(\eta, \varsigma) \right]^2, \tag{7}$$

The value of λ was chosen as 1.0×10^6 in this work.

3 Fuzzy logic control (FLC) for adaption of penalty coefficient

The membership functions (MFs) used for the input and output variables to the FLC are shown in Figs. 2 and 3, respectively. In which, according to the interpretation of the fuzzy linguistic terms (Zadeh 1965), the following five fuzzy variables were used in this study: very small (VS), small (S), medium (M), large (L) and very large (VL).

The rule-based fuzzy inference system shown in Table 1 is determined based on the Mamdani Model, the structure of which is the popular system of multi-input single output (MISO).

Following lists the procedure in determining the $FLC(\eta, \xi)$.

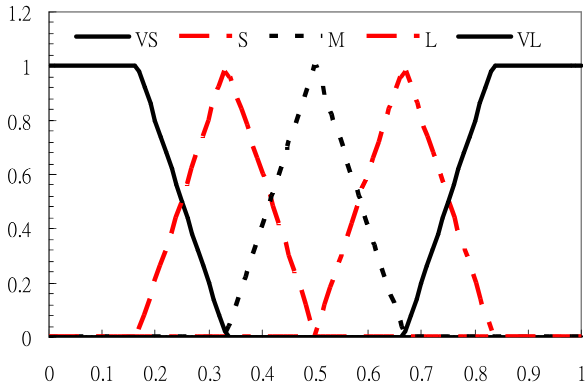

Fig. 2 MFs for the input variable

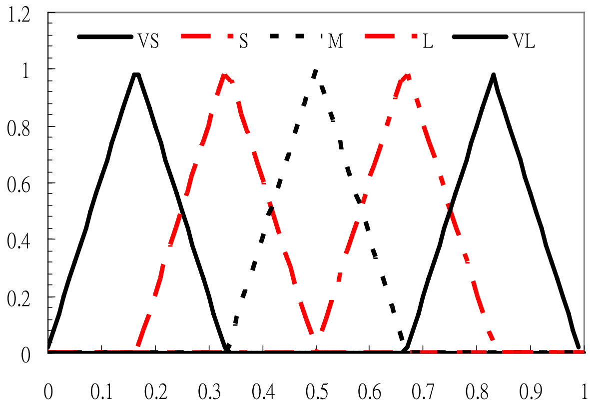

Fig. 3 MFs for the output variable

Table 1 The rule-based fuzzy inference system

	ξ				
η	**VS**	**S**	**M**	**L**	**VL**
VS	**VS**	**VS**	**VS**	**S**	**M**
S	**VS**	**VS**	**S**	**M**	**L**
M	**VS**	**S**	**M**	**L**	**VL**
L	**S**	**M**	**L**	**VL**	**VL**
VL	**M**	**L**	**VL**	**VL**	**VL**

1. Determine the membership values corresponding to the input η and ξ

$$\mathrm{Poss}(A_{i1}|\eta) = \max_{x_1 \in U_1} (A_{i1}(x_1) \wedge \eta) \quad i = 1\text{--}5 \tag{8}$$

$$\mathrm{Poss}(A_{i2}|\xi) = \max_{x_2 \in U_2} (A_{i2}(x_2) \wedge \xi) \quad i = 1\text{--}5 \tag{9}$$

where $i = 1$–5 corresponds to five fuzzy variables of VS, S, M, L and VL, respectively, η and ξ are fuzzy singletons, x_1 and x_2 are the underlying domains between

0 to 1 corresponding to normalized coefficients η and ξ, respectively, and $A_{i1}(x_1)$ and $A_{i2}(x_2)$ are input MFs as shown in Fig. 2.

2. Find the maximum of the two values above

$$\tau_i = \text{Poss}(A_{i1}|\eta) \cap \text{Poss}(A_{i2}|\xi) \quad i = 1\text{–}5 \tag{10}$$

3. Find the output fuzzy function corresponding to each τ_i

$$R_i(y) = \tau_i \wedge B_i(y) \quad i = 1\text{–}5 \quad \forall y \in Y \tag{11}$$

where $B_i(y)$ is the output MFs as shown in Fig. 3 and Y is the universe of discourse between 0 to 1 representing the normalized output domain space.

4. Aggregate the output fuzzy functions

$$R(y) = \bigcup_{i=1}^{5} R_i(y) = R_1(y) \cup R_2(y) \cup \cdots \cup R_5(y), \quad \forall y \in Y \tag{12}$$

5. Defuzzify the aggregated output fuzzy function to find the scale factor $FLC(\eta, \xi)$ of the penalty coefficient based on center of gravity method (COG) (Zadeh 1965).

$$FLC(\eta, \xi) = \frac{\sum_{i=1}^{5} b_i^* \sum_{j=1}^{N} R_i(y_j)}{\sum_{i=1}^{5} \sum_{j=1}^{N} R_i(y_j)} \tag{13}$$

where N is the number of intervals in calculating the summation of aggregated output fuzzy functions, which is adopted as $N = 100$ here, and b^* is the centroid of the output fuzzy functions.

4 Genetic algorithm (GA) as optimization solver

Equations (7) is used as the fitness function of the GA, the chromosomes with higher fitness values have a greater chance to be selected into the mating pool. The probability of the i-th chromosome $\mathbf{x}_i$, the vector indicating the design variables illustrated previously, being selected is

$$P(\mathbf{x}_i) = \frac{F(\mathbf{x}_i)}{\sum_{j=1}^{N} F(\mathbf{x}_j)} \tag{14}$$

where N is the population size. The real values, rather than the binary encoding, of the continuous variables were employed directly. The cross-over method of generating the children chromosome $\mathbf{x}_{new}$, the vector indicating the design variables of the new generation, is based on a combination of the parents, i.e.,

$$\mathbf{x}_{new} = \gamma \mathbf{x}_{ma} + (1 - \gamma)\mathbf{x}_{da} \tag{15}$$

where γ is a random number on the interval [0, 1], and $\mathbf{x}_{ma}$ and $\mathbf{x}_{da}$ are the vectors of design variable vectors of the mother chromosome and father chromosome, respectively.

The mutation is performed by adding a normally distributed random number to the variable selected as follows

$$x_i' = x_i + \sigma N(0, 1) \tag{16}$$

where σ is the standard deviation of the normal distribution, $N(0, 1)$ is the standard normal distribution with zero mean and variance equal to 1 (Haupt and Haupt 2004), and x_i is the i-th gene indicating the i-th design parameter of the design vector $\mathbf{x}$.

In this paper, six significant factors sensitive to the analytical results of the GA, which include the chromosome number, the size of the population, the maximum number of the iterative generation, the fraction rate of the kept population, the crossover rate and the mutation rate, were set to be adapted flexibly to enhance the efficiency of the calculations (Haupt and Haupt 2004).

5 Investigations of the proposed algorithm

Figure 4 shows the flowchart of the proposed algorithm. In order to investigate the algorithm, the reported results of cyclic loading tests on three RC columns (Nagaya and Kawashima 2001; Chang and Chang 1999; Chung 2000) were employed as case studies, in which a square section, a rectangular section, and a circular section of the columns were involved. Table 2 contains the details of the experiments. All of the real capacity curves enveloping the experimental hysteretic loops were taken into account as the targets of these designs. Four important parameters, which include the yielding displacement δ_Y, the yielding force P_Y, the ultimate displacement δ_U, and the ultimate force P_U, were taken into account as the design objectives for our optimal model. All the specimens were modeled structurally as a cantilever column for the pushover analysis.

The design parameters, such as the size of the column section (b, h or D), the number of longitudinal reinforcements (n_L, n_S), the diameter of the longitudinal reinforcement (D_L), the spacing of the transverse reinforcement (m) and the diameter of the transverse reinforcement (D_T), were set as discrete design variables, whereas others the continuous design variables.

Case 1: Square section of RC pier

Based on the experimental result, the design objectives selected were the yielding displacement $\delta_{Y,\,\text{squared}} = 10$ mm, the yielding force $P_{Y,\,\text{squared}} = 130$ kN, the ultimate displacement $\delta_{U,\,\text{squared}} = 50$ mm, and the ultimate force $P_{U,\,\text{squared}} = 135$ kN.

Six analytical results of the design, obtained from the proposed procedure, represented by the ten design parameters of the squared RC pier are listed in Table 3. Figure 5 shows the dimensions of the specimen (Nagaya and Kawashima 2001) and shows the corresponding capacity curves via the pushover analyses of the six designs. These curves are found to be in good agreement with the envelope of the experimental hysteretic loop. Table 3 shows that the costs of the design result-3, result-5 and result-6 are about 92% of that of specimen-1, among which, the design result-5 has the minimum cost and can be regarded as the optimal solution.

Case 2: Rectangular section of RC pier

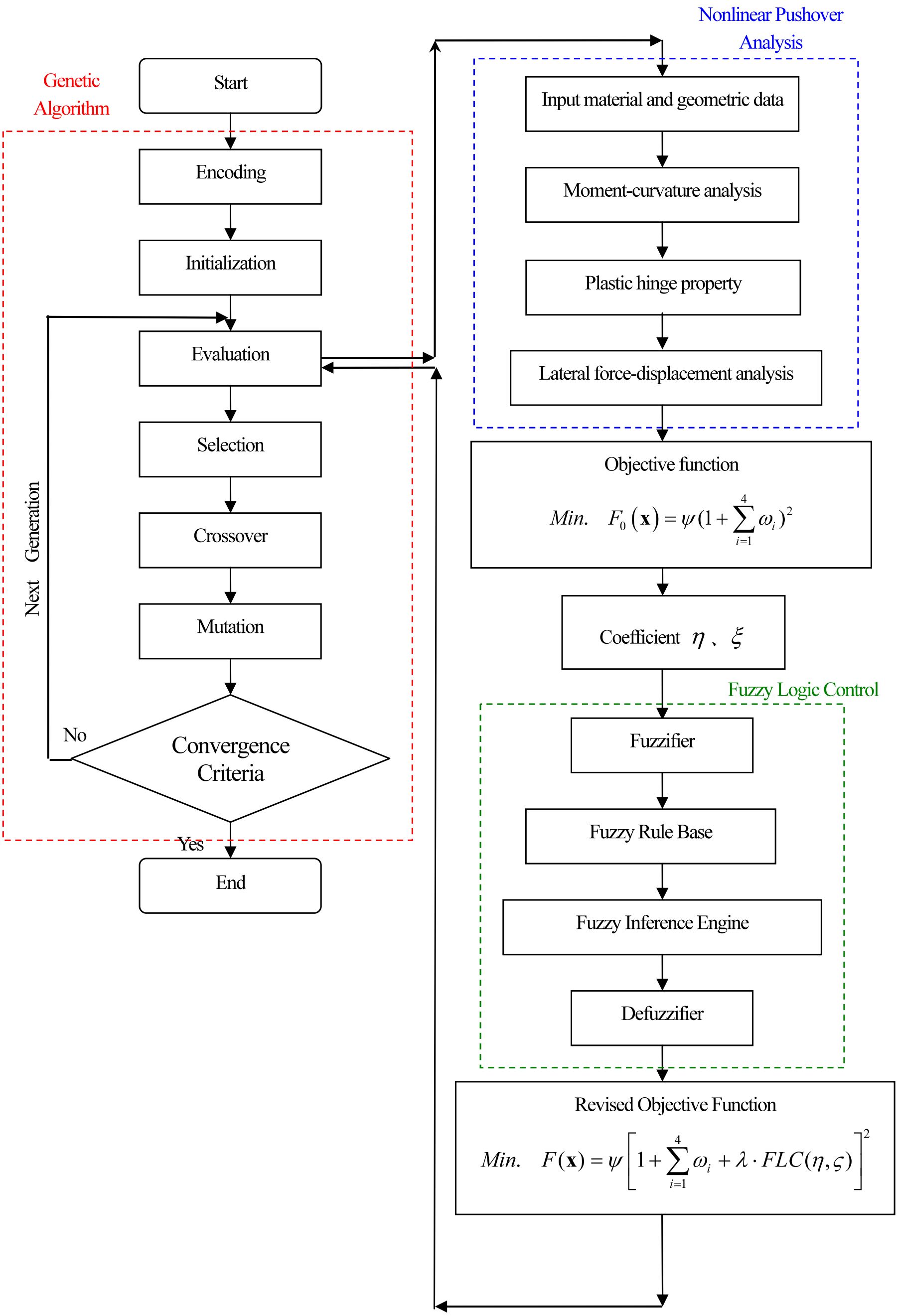

Fig. 4 Flowchart of the proposed algorithm

Table 2 Details of specimens for cyclic loading tests of RC column (Kelesoglu 2007; Zou and Chan 2005; Haupt and Haupt 2004) (Nagaya and Kawashima, 2001; Chang and Chang, 1999; Chung, 2000)

	Unit	Specimen 1 Square section	Specimen 2 Rectangular section	Specimen 3 Circular section
Concrete compression stress f_c'	MPa	29.4	22.05	26
Yielding stress of longitudinal reinforcement f_y	MPa	372	436.8	490.5
Yielding stress of transverse reinforcement f_{yh}	MPa	363	450.8	490.5
Yielding stress of tie reinforcement f_{yt}	MPa	–	450.8	490.5
Cross section	mm	400 × 400	600×750	Diameter 760
Height	mm	1350	3250	3250
Cover	mm	27.5	25	25
Arrangement of longitudinal reinforcement	–	20-D13	32-D19	34-D19
Spacing of transverse reinforcement	mm	D6@50	D10@100	D10@70
Spacing of tie reinforcement along the long side	mm	–	2-D10@100	1-D10@70
Spacing of tie reinforcement along the short side	mm	–	3-D10@100	1-D10@70-
Axial load (kN)	kN	157	1400	1400
Total Cost	NT dollars	24,082.0	92,432.0	108,240.0

Table 3 Six design results of the square RC pier

Designed results	Result - 1	Result - 2	Result - 3	Result - 4	Result - 5	Result - 6
Section (mm)	350×350	400×400	350×350	350×350	350×350	450×450
Arrangement of Longitudinal Reinforcement	24-D13	16-D16	20-D16	24-D13	12-D19	20-D13
(Section Ratio)	(2.60%)	(2.01%)	(3.28%)	(2.60%)	(2.78%)	(1.31%)
Arrangement of Transverse reinforcement	D10@50 mm	D6@50 mm	D6@50 mm	D10@50 mm	D10@100 mm	D10@50 mm
Strength of concrete (MPa)	30.4	30.3	25.9	30.0	25.3	23.8
Strength of Longitudinal Reinforcement (MPa)	410.2	329.4	330.5	407.8	398.4	313.5
Strength of Transverse reinforcement (MPa)	381.8	407.5	411.9	344.5	399.5	337.3
Total Cost (NT dollars)	26,289.0	25,031.0	22,063.0	25,789.0	22,045.0	22,167.0
$\frac{\cos t\_\mathrm{result}}{\cos t\_\mathrm{specimen\_1}}$	1.09	1.04	0.92	1.07	0.92	0.92

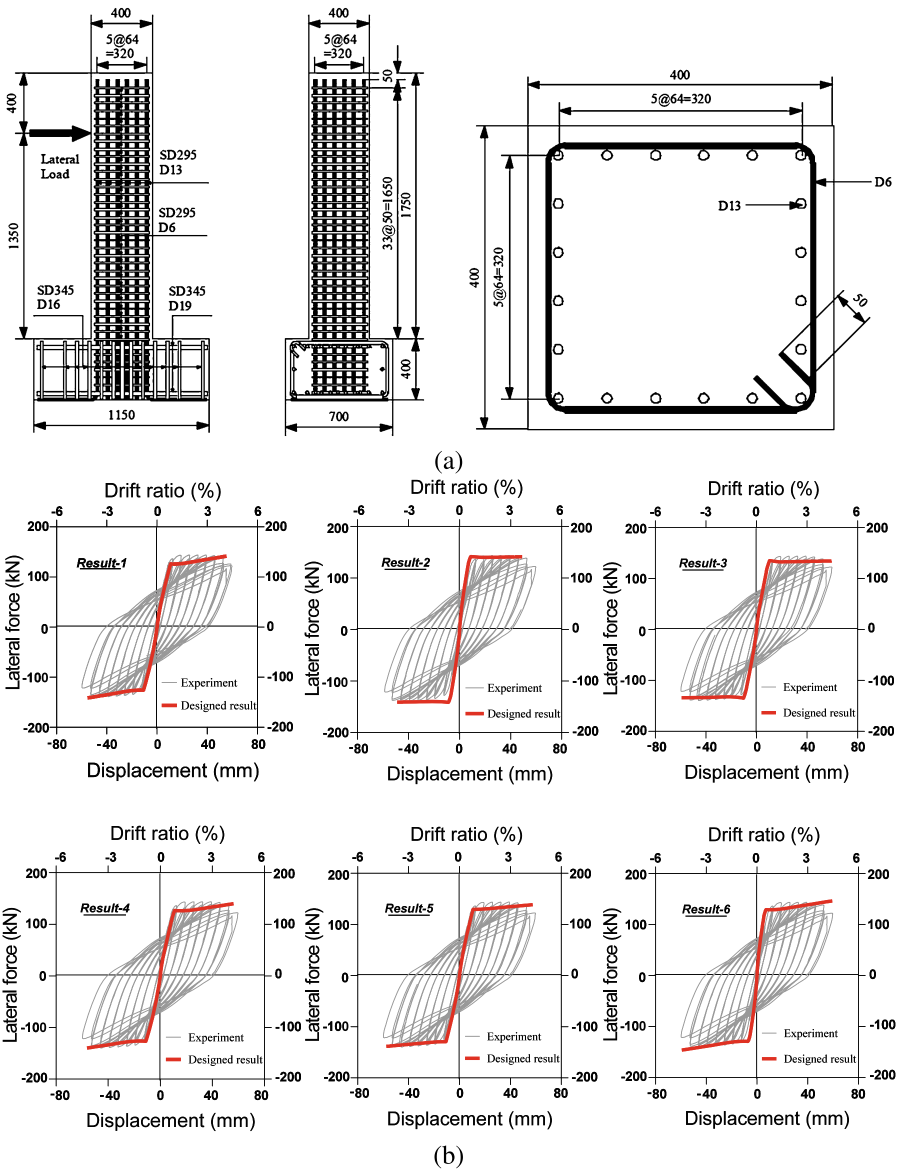

Fig. 5 (**a**) Specimen 1 (Kelesoglu 2007). (Nagaya and Kawashima, 2001). (**b**) Comparison between the pushover analyses of the six designs obtained and the experimental hysteretic loop of the square specimen

Based on the experimental result, the design objectives selected were the yielding displacement $\delta_{Y,\,\mathrm{rectangular}} = 40$ mm, the yielding force $P_{Y,\,\mathrm{rectangular}} = 430$ kN, the ultimate displacement $\delta_{U,\,\mathrm{rectangular}} = 180$ mm and the ultimate force $P_{U,\,\mathrm{rectangular}} = 410$ kN.

Six analytical results of the design represented by the ten design parameters of the rectangular RC pier are listed in Table 4. Figure 6 shows the dimensions of the

Table 4 Six design results of the rectangular RC pier

Designed results	Result - 1	Result - 2	Result - 3	Result - 4	Result - 5	Result - 6
Section (mm)	600×800	600×750	600×800	600×750	600×750	600×800
Arrangement of Longitudinal Reinforcement	34-D16	32-D19	34-D16	32-D19	32-D19	36-D16
(Section Ratio)	(1.42%)	(2.01%)	(1.42%)	(2.01%)	(2.01%)	(1.51%)
Arrangement of Transverse reinforcement	D10@100 mm	D10@100 mm	D10@100 mm	D10@100 mm	D10@100 mm	D10@100 mm
Strength of concrete (MPa)	22.6	25.9	22.1	23.3	21.6	20.9
Strength of Longitudinal Reinforcement (MPa)	474.9	434.7	480.5	433.2	434.4	478.1
Strength of Transversal reinforcement (MPa)	463.5	460.1	452.2	467.7	465.5	439.3
Total Cost (NT dollars)	86,713.0	96,870.0	85,475.0	90,896.0	86,945.0	83,402.0
$\frac{\cos t\_\text{result}}{\cos t\_\text{specimen\_2}}$	0.94	1.05	0.92	0.98	0.94	0.90

Fig. 6 (**a**) Specimen 2 (Zou and Chan 2005) (Chang and Chang, 1999). (**b**) Comparison between the pushover analyses of the six designs obtained and the experimental hysteretic loop of the rectangular specimen

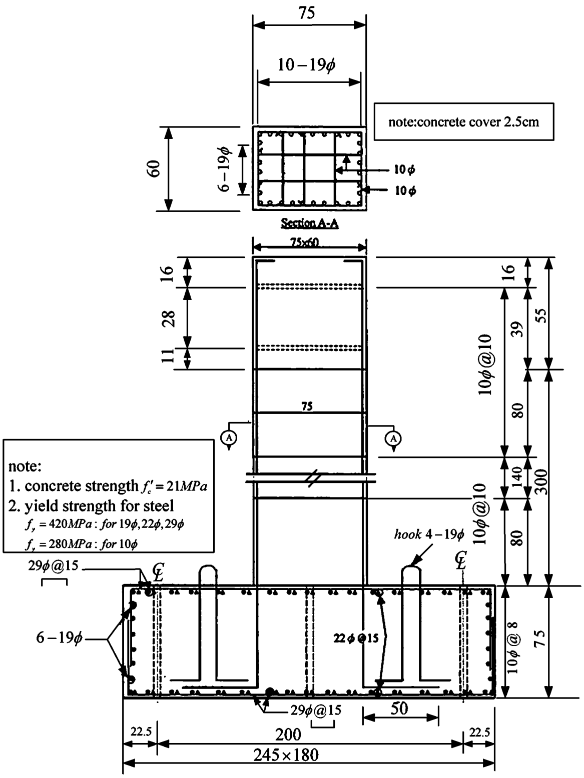

(a)

specimen (Chang and Chang 1999) and shows the corresponding capacity curves via the pushover analyses of the six designs. These curves are found to be in good agreement with the envelope of the experimental hysteretic loop. Table 4 shows that the cost of design result-6 is about 90% of that of specimen-2 and is the minimum one of the six results, therefore, it can be regarded as the optimal solution.

Case 3: Circular section of RC pier

Based on the experimental result, the design objectives selected were the yielding displacement $\delta_{Y,\,\text{circular}} = 45$ mm, the yielding force $P_{Y,\,\text{circular}} = 480$ kN, the ultimate displacement $\delta_{U,\,\text{circular}} = 165$ mm, and the ultimate force $P_{U,\,\text{circular}} = 470$ kN.

Six analytical results of the design represented by the eight design parameters of the circular RC pier are listed in Table 5. Figure 7 shows the dimensions of the specimen (Chung 2000) and shows the corresponding capacity curves via the pushover analyses of the six designs. These curves are found to be in good agreement with the envelope of the experimental hysteretic loop. Table 5 shows that the cost of design result-1 is about 89% of that of specimen-3 and is the minimum one of the six results, therefore, it can be regarded as the optimal solution.

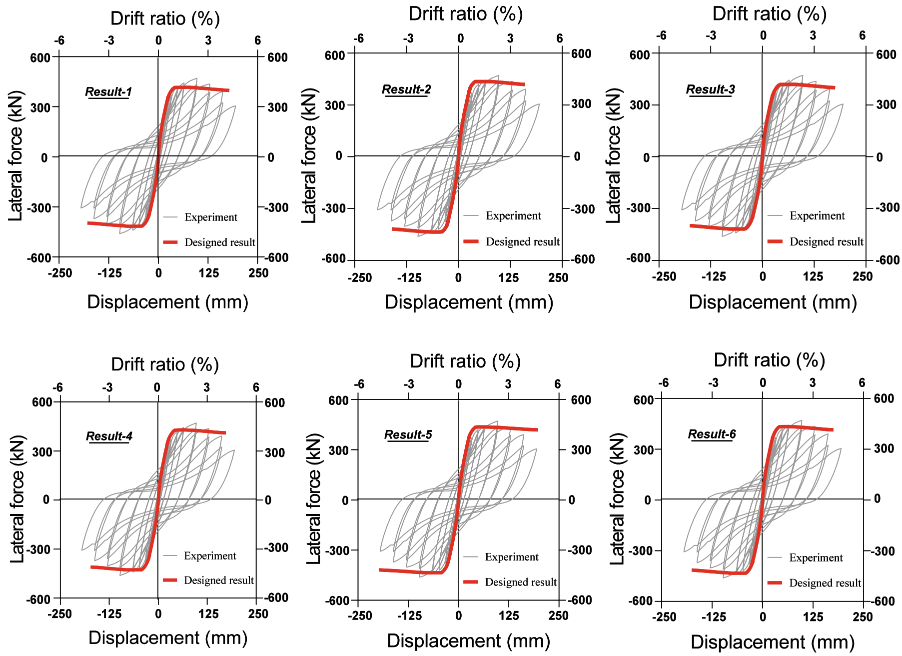

(b)

Fig. 6 (*Continued*)

6 Discussions

Since these designs are inverse problems, the solution of every problem will not be unique. It can be seen that the design parameters obtained from the algorithm are not exactly the same as those of the experiments, however, they are all feasible solutions because the corresponding capacity curves from the pushover analyses of these designs are consistent with the envelopes of the experimental hysteretic loops. As a result, the utility of the proposed algorithm has been demonstrated.

7 Case study on PBSD of a square RC bridge pier

A square RC bridge pier with a height of 6 m was modeled structurally as show in Fig. 8. Because the pier and superstructure are separate, it was modeled as a cantilever column with a lumped mass at the top. The pier was subjected to four performance objectives (fully operational, operational, life safety and near collapse) with respect to different levels of earthquake shown in Table 6. The peak ground accelerations (PGAs): 0.12 g, 0.18 g, 0.30 g and 0.40 g corresponding to the return periods of the earthquake: $T_r = 30$ yr, $T_r = 75$ yr, $T_r = 475$ yr, and $T_r = 2500$ yr, respectively, were determined based on the seismic hazard analysis at the bridge site. On the basis of the displacement-based design method (Xue and Wu 2006), the corresponding spectral displacements S_ds can be specified and listed. Suppose that the S_d of the

Table 5 Six design results of the Circular RC pier

Designed results	Result - 1	Result - 2	Result - 3	Result - 4	Result - 5	Result - 6
Diameter (mm)	780	760	780	740	800	800
Arrangement of Longitudinal Reinforcement	34-D19	34-D19	32-D19	36-D19	30-D19	30-D19
(Section Ratio)	(2.02%)	(2.13%)	(1.90%)	(2.37%)	(1.69%)	(1.69%)
Arrangement of Transverse reinforcement	D10@70 mm	D10@70 mm	D10@70 mm	D10@60 mm	D10@60 mm	D10@60 mm
Strength of concrete (MPa)	21.2	25.7	28.2	28.7	31.8	25.6
Strength of Longitudinal Reinforcement (MPa)	480.6	487.9	481.0	478.2	479.9	501.9
Strength of Transversal reinforcement (MPa)	490.3	510.0	504.0	481.0	504.3	471.7
Total Cost (NT dollars)	96,605.0	107,792.0	114,384.0	115,952.0	127,091.0	109,972.0
$\frac{\cos t\_\text{result}}{\cos t\_\text{specimen\_3}}$	0.89	1.00	1.06	1.07	1.17	1.02

Fig. 7 (**a**) Specimen 3 (Haupt and Haupt 2004) (Chung, 2000). (**b**) Comparison between the pushover analyses of the six designs obtained and the experimental hysteretic loop of the circular specimen

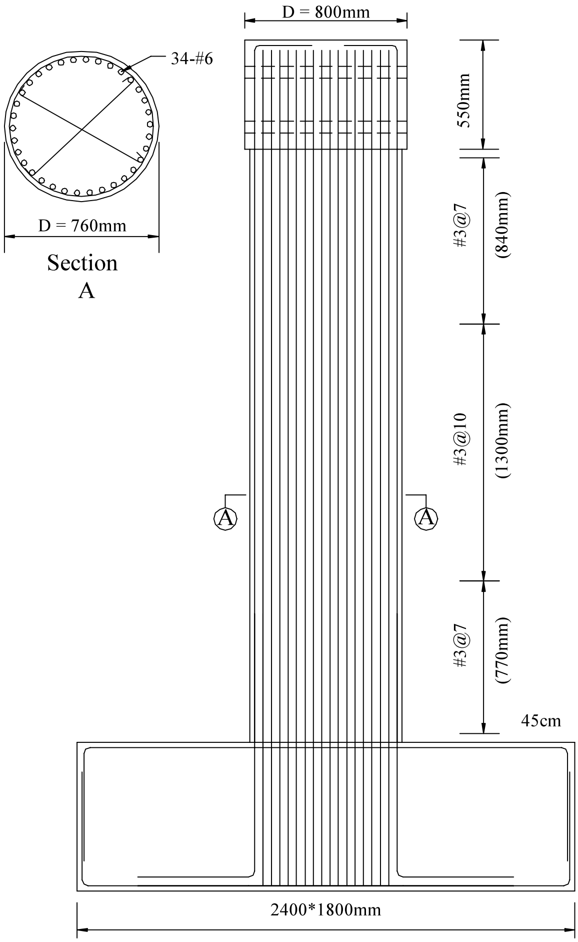

(a)

second performance objective PO_2 was regarded as the yield spectral displacement, i.e. $S_{d2} = S_{dy}$, the ductility ratio of the spectral displacement for each performance objective can be calculated accordingly and represented by $\mu = (S_{di}/S_{dy})$, $i = 1$–4.

Sung et al. selected more than two hundred ground motions recorded in the Chi–Chi earthquake (Chang 1999) as the seismic inputs for the time history analyses of two SDOF systems where one is a bi-linear system and the other is a linear one with identical mass, viscous damping and elastic stiffness. The responses of these two systems are shown in Fig. 9. According to the analyses, the following formulations have been regressed (Sung et al. 2007):

$$\Omega = \left[\mu - (\mu - 1)\exp\left(\frac{-a}{\mu^b}\right)\right] \tag{17}$$

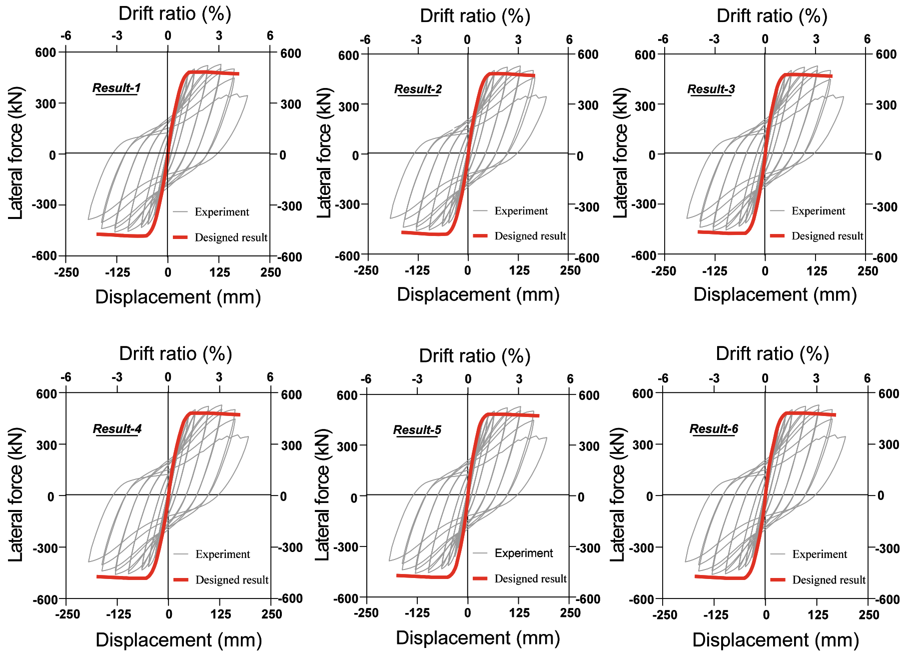

(b)

Fig. 7 (*Contuinued*)

Fig. 8 Square RC bridge pier

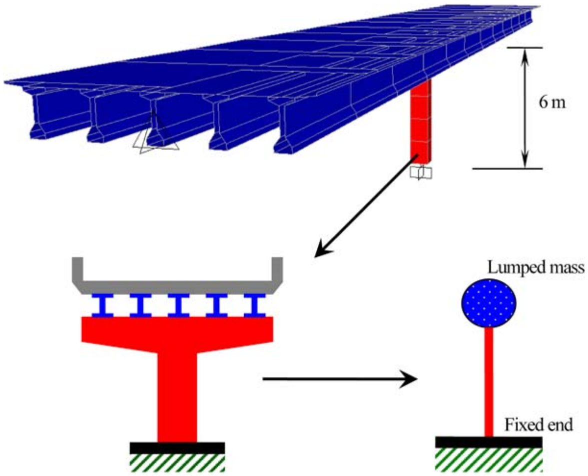

where $\Omega = S_{ae}/S_{ay}$ is the ratio of the elastic pseudo spectral acceleration S_{ae} of the linear system to the pseudo spectral yield acceleration S_{ay} of the bi-linear system when the two systems are subjected to the same seismic excitation. On the other hand, $\mu = (S_{di}/S_{dy})$ is the ratio of the inelastic spectral displacement S_{di} to the spectral yield displacement S_{dy} of the bi-linear system. The coefficients a and b are

Table 6 Performance objectives of the RC bridge column

	Fully Operational PO_1	Operational PO_2	Life Safety PO_3	Near Collapse PO_4
PGA	0.12 g ($T_r = 30$ yr)	0.18 g ($T_r = 75$ yr)	0.30 g ($T_r = 475$ yr)	0.40 g ($T_r = 2500$ yr)
S_d	2.80 cm	3.70 cm	12.00 cm	17.50 cm
μ[a]	0.75	1.00	3.25	4.73

[a]Ductility ratio, $\mu = (S_{di}/S_{dy})$

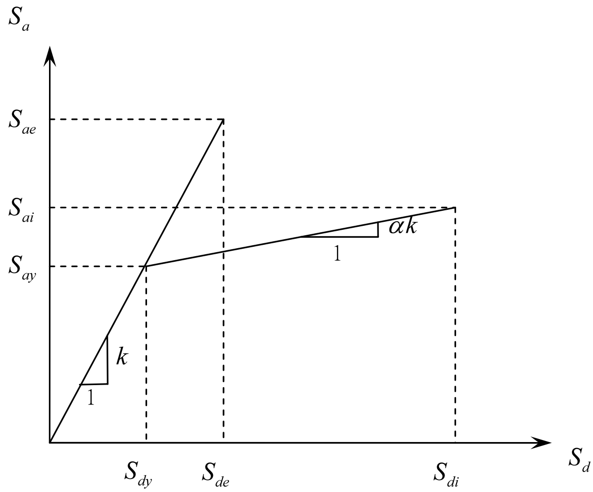

Fig. 9 Relationship between Linear and Bi-linear SDOF Systems

the parameters dependent upon the fundamental period of the structure T, the soil condition, and the post-yield stiffness ratio α.

According to the bridge design code in Taiwan, the ratio of the normalized elastic pseudo acceleration response spectrum to gravity acceleration, for the soil condition considered, is expressed as:

$$C = 1.5/T^{2/3} \quad \text{for } 0.465 \text{ sec} \le T \le 1.315 \text{ sec} \tag{18}$$

Therefore, the elastic pseudo spectral acceleration can be written as

$$S_{ae} = PGA \times C = PGA \times 1.5/T^{2/3} \quad \text{for } 0.465 \text{ sec} \le T \le 1.315 \text{ sec} \tag{19}$$

Based on the performance objectives PO_1 and PO_2, the fundamental period of the pier can be determined by the following equation

$$T = \min_j \left(2\pi \sqrt{\frac{S_{dj}}{(S_{ae})_j}} \right), \quad j = 1, 2 \tag{20}$$

In this case, the calculated fundamental period is $T = 0.64$ sec, and the pseudo spectral yield acceleration is given as

$$S^*_{ay} = \left(\frac{2\pi}{T}\right)^2 S_{dy} = \left(\frac{2\pi}{0.64}\right)^2 \times 3.70 = 356\ \text{cm/sec}^2 \tag{21}$$

Assuming that the post-yield stiffness ratio is $\alpha = 0.01$, and the coefficients are $a = 1.563$ and $b = 0.595$, in (17), can be found in the reported results (Sung et al. 2007). As a result, the Ω_3 and the Ω_4 with respective to PO_3 and PO_4 can be obtained as

$$\begin{aligned}\Omega_3 &= \left[\mu_3 - (\mu_3 - 1)\exp\left(\frac{-a}{\mu_3^b}\right)\right] \\ &= \left[3.25 - (3.25 - 1)\exp\left(\frac{-1.307}{3.25^{0.602}}\right)\right] = 2.07,\end{aligned} \tag{22}$$

$$\begin{aligned}\Omega_4 &= \left[\mu_4 - (\mu_4 - 1)\exp\left(\frac{-a}{\mu_4^b}\right)\right] \\ &= \left[4.73 - (4.73 - 1)\exp\left(\frac{-1.307}{4.73^{0.602}}\right)\right] = 2.50.\end{aligned} \tag{23}$$

The pseudo spectral acceleration reduction factor $SAR = S_{ai}/S_{ae}$ relates to Ω as

$$SAR = \frac{1}{\Omega}[1 + \alpha(\mu - 1)] \tag{24}$$

The SAR_3 and SAR_4 with respect to PO_3 and PO_4 can be obtained as

$$SAR_3 = \frac{1}{\Omega_3}[1 + \alpha(\mu_3 - 1)] = \frac{1}{2.07}[1 + 0.01 \times (3.25 - 1)] = 0.49 \tag{25}$$

$$SAR_4 = \frac{1}{\Omega_4}[1 + \alpha(\mu_4 - 1)] = \frac{1}{2.50}[1 + 0.01 \times (4.73 - 1)] = 0.41 \tag{26}$$

The inelastic pseudo spectral acceleration $(S_{ai})_3$ and $(S_{ai})_4$ with respect to PO_3 and PO_4 can be given as

$$\begin{aligned}(S_{ai})_3 &= SAR_3 \times (S_{ae})_3 = SAR_3 \times PGA_3 \times C \\ &= 0.49 \times 0.3 \times 980 \times 1.5/0.64^{2/3} = 291\ \text{cm/sec}^2\end{aligned} \tag{27}$$

$$\begin{aligned}(S_{ai})_4 &= SAR_4 \times (S_{ae})_4 = SAR_4 \times PGA_4 \times C \\ &= 0.41 \times 0.4 \times 980 \times 1.5/0.64^{2/3} = 325\ \text{cm/sec}^2\end{aligned} \tag{28}$$

The pseudo spectral yield acceleration $(S_{ay})_3$ and $(S_{ay})_4$ with respect to PO_3 and PO_4 can be estimated as

$$(S_{ay})_3 = \frac{(S_{ai})_3}{1 + \alpha(\mu_3 - 1)} = \frac{291}{1 + 0.01 \times (3.25 - 1)} = 285\ \text{cm/sec}^2 \tag{29}$$

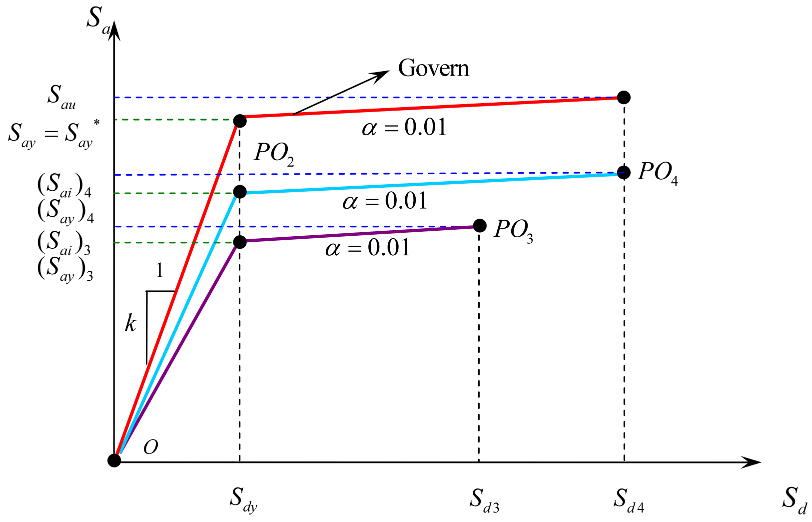

Fig. 10 The capacity spectrum of the target column

$$(S_{ay})_4 = \frac{(S_{ai})_4}{1 + \alpha(\mu_4 - 1)} = \frac{325}{1 + 0.01 \times (4.73 - 1)} = 313 \text{ cm/sec}^2 \tag{30}$$

Finally, the pseudo spectral yield acceleration of the bridge pier can be chosen as the maximum of S_{ay}^*, $(S_{ay})_3$, and $(S_{ay})_4$, i.e.

$$S_{ay} = \max[S_{ay}^*,\ (S_{ay})_3,\ (S_{ay})_4] = [356,\ 285,\ 313] = 356 \text{ cm/sec}^2 \tag{31}$$

The pseudo spectral ultimate acceleration of the pier is

$$S_{au} = S_{ay}[1 + \alpha(\mu - 1)] = 356 \times [1 + 0.01(4.73 - 1)] = 369 \text{ cm/sec}^2 \tag{32}$$

The properties of a bilinear system that relate S_a and S_d (capacity spectrum) as shown in Fig. 10, characterized by the calculated $S_{ay} = 356$ cm/sec^2, $S_{dy} = 3.69$ cm, $S_{au} = 369$ cm/sec^2 and $S_{du} = 17.45$ cm, cannot simultaneously satisfy all the specified performance objectives, however, it is in agreement with the extreme requirements among the objectives and therefore can be adopted for practical design. Based on the theory of structural dynamics, the capacity spectrum can then be transferred into the capacity curve (ACI Committee 318x 2005) represented by $P_Y = 5{,}059$ kN, $\delta_Y = 48$ mm, $P_U = 5{,}244$ kN and $\delta_U = 192$ mm, as shown in Fig. 11, which is able to be taken into account as the design target of the pier.

To simplify the design, the strength of concrete was fixed to be $f_c' = 34.3$ MPa, the strength of longitudinal reinforcement together with transverse reinforcement was set to be the same $f_y = f_{yh} = 411.8$ MPa, and the spacing of the transverse reinforcement $s = 100$ mm, which are all usually employed by engineers for RC structural design. The number of the longitudinal reinforcements $n = n_L = n_S$, the diameter of the longitudinal reinforcement D_L, and the diameter of the transverse reinforcement D_T were set to be discrete design variables. Based on the proposed algorithm,

Table 7 Details of six design results of the RC column

Designed results	Design - 1	Design - 2	Design - 3	Design - 4	Design - 5	Design - 6
Section (mm)	1500×1500	1550×1550	1600×1600	1650×1650	1700×1700	1750×1750
Arrangement of Longitudinal Reinforcement	104-36φ	96-36φ	112-32φ	104-32φ	112-29φ	120-29φ
(Section Ratio)	(4.70%)	(4.07%)	(3.52%)	(3.07%)	(2.56%)	(2.59%)
Arrangement of Transversal reinforcement	19φ@100 mm	19φ@100 mm	19φ@100 mm	19φ@100 mm	19φ@100 mm	22φ@100 mm
Strength of Concrete (MPa)			34.3			
Strength of Longitudinal Reinforcement (MPa)			411.8			
Strength of Transversal reinforcement (MPa)						
Total Cost (NT dollars)	1,717,770.0	1,651,810.0	1,617,190.0	1,570,500.0	1,458,220.0	1,627,190.0

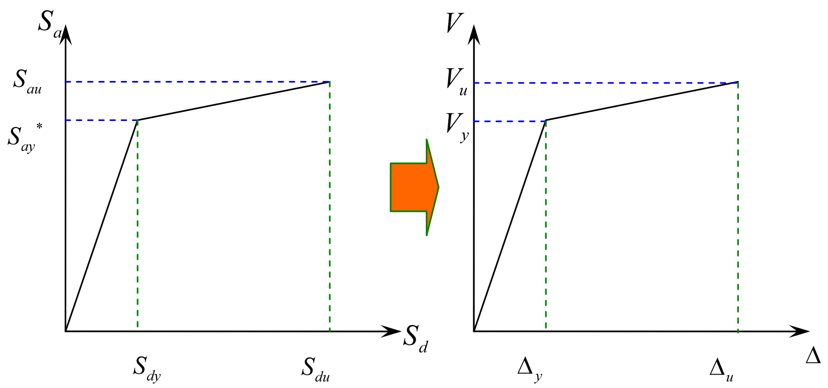

Fig. 11 The capacity curve of the target column

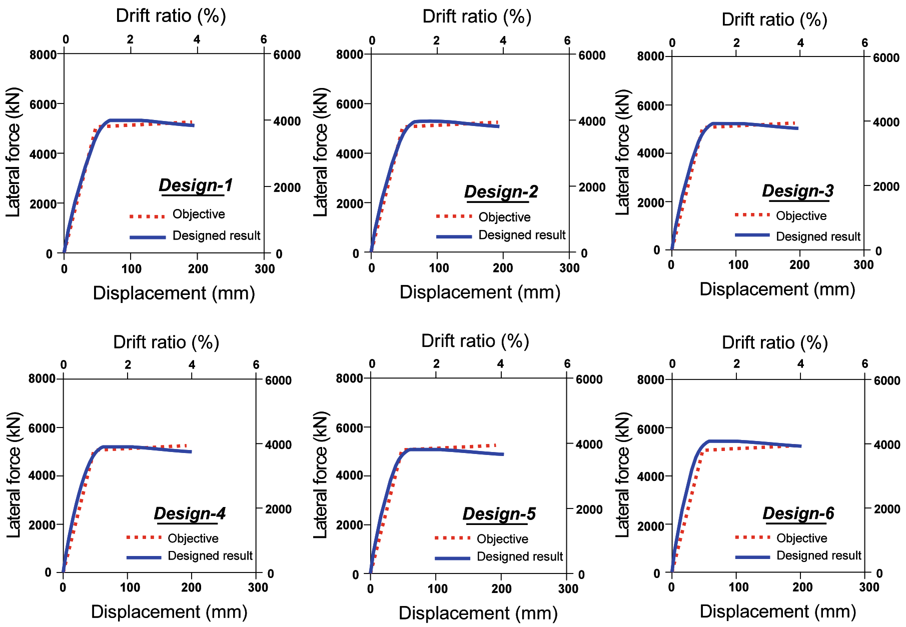

Fig. 12 Comparison between the pushover analyses of the six designs obtained and the designed capacity curve

six design results shown in Table 7 were obtained and their corresponding pushover analyses associated with the specified design target are shown in Fig. 12. It is clear that the discrepancy between each analysis result and the target seem to be insignificant and the designs fulfill the specified requirements.

Table 7 shows the construction cost as well as the design parameters of the six pier sections obtained. All the design results satisfy the specifications of the design code. It can be seen that the result of the Design-5 with the minimum construction cost of NT$ 1,458,220.0 is the optimal one.

8 Conclusions

Based on the analyses presented in this paper, the following conclusions may be made:

1. The performance-based seismic design (PBSD) of the RC bridge pier with single-column type can be modeled as a constrained optimization problem with the objective of minimizing construction cost and constraints of multiple-level structural performance with respect to different levels of earthquake together with the limitations on the arrangement of reinforcements specified in the seismic design code for RC structures. The penalty for violating the constraints were combined with construction cost to serve as the objective function of the optimization algorithm. Since the model cannot be formulated in an explicit mathematical function, a genetic algorithm (GA) with a penalty function was chosen to be the optimization solver.
2. Fuzzy logic control (FLC), based on the fuzzy inference system with the structure of multi-input single output (MISO), was implemented to adapt the penalty coefficient to prevent the penalty from being too weak or too strong through the entire calculation of the GA. The individual superiority of the GA and the FLC were developed significantly through the proposed approach.
3. The reported results of cyclic loading tests of three RC columns served as the data base for the necessary investigations. The envelopes of the experimental hysteretic loops were used as the target bi-linear systems. For every target, six design results were obtained from the proposed algorithm and their corresponding capacity curves were calculated from a pushover analysis. The design parameters obtained were not found to be exactly the same as those of the experimental specimens, however, their corresponding capacity curves were consistent with the envelopes of the real hysteretic loops of the experiments. This shows the utility of the proposed algorithm.
4. The authors' previous study on the seismic requirements with respect to different levels of earthquake, using a time history analysis of more than two hundred ground motions recorded in the Chi–Chi earthquake (1999, Taiwan) as the seismic inputs, was employed to implement the multiple performance objectives in the PBSD. The present proposed algorithm completed the whole procedure of the PBSD for the RC bridge columns. It shows that the design results can satisfy the extreme cases of the four different performance objectives (fully operational, operational, life safety and near collapse) commonly used as the design principle of the PBSD. From the results obtained, the optimal one with minimum construction cost can be chosen. The systematic design procedure we propose can avoid man-made discrepancy and enhance the design precision of the PBSD.
5. This paper is focused on the PBSD of an RC bridge pier with single-column type. The pushover analysis is applied on a modeled cantilever structure with either a vertical centric or eccentric dead load. This study is essential for the PBSD of the entire bridge structure. Because all the bearings and the piers can be modeled as substructures of the whole bridge system in cases where the structural nonlinearities are given, an equivalent bilinear system of spring elements can be modeled to represent the structural nonlinearities of the piers or the bearings, and

linked to the beam elements representing the girders of the bridge. Accordingly, the whole bridge system can be simplified and the pushover analysis performed easily. The fuzzy genetic algorithm can also be used to solve this PBSD problem and give a good solution search to determine the optimal structural nonlinearities of the equivalent spring elements to satisfy various performance requirements of the bridge system. As a result, the required structural nonlinearities of the piers can be obtained and their detailed designs can be completed through the proposed processes.

Acknowledgements The financial supports received from the National Science Council, Taipei, Taiwan, through Grants No. NSC-94-2625-Z-027-004 and No. NSC-95-2625-Z-027-003 are gratefully acknowledged.

References

ACI Committee 318x (2005) Building code requirements for reinforced concrete and commentary (ACI 318-05), American Concrete Institute, Farmington Hill, USA

ATC-40 (1996) Seismic Evaluation and Retrofit of Concrete Building, Applied Technology Council, Redwood City, California

Bazaraa MS, Shetty CM (1979) Nonlinear programming: theory and algorithms. Wiley, New York

Chang KC (1999) Seismic investigation of bridge damage in Chi–Chi Earthquake. Report no NCREE-90-055, National Center for Research on Earthquake Engineering, Taipei, Taiwan

Chang KC, Chang HF (1999) Seismic retrofit study of rectangular bridge column with CFRP jackets. Report no NCREE-00-030, National Center for Research on Earthquake Engineering, Taipei, Taiwan

Chung LL (2000) Seismic retrofit study of RC bridge columns. Report no NCREE-00-035, National Center for Research on Earthquake Engineering Taipei, Taiwan

Harp DR, Taha MR, Ross TJ (2009) Genetic-fuzzy approach for modeling complex systems with an example application in masonry bond strength prediction. J Comput Civil Eng 23:193–199

Haupt RL, Haupt SE (2004) Practical genetic algorithms, 2nd edn. Wiley, New Jersey

Kelesoglu O (2007) Fuzzy multiobjective optimization of truss-structures using genetic algorithm. Adv Eng Softw 38:717–721

Nagaya K, Kawashima K (2001) Effect of aspect ratio and longitudinal reinforcement diameter on seismic performance of reinforced concrete bridge columns. Report no TIT/EERG 01, Institute of Technology, Tokyo, Japan

Nanakorn P, Messomklin K (2001) An adaptive penalty function in genetic algorithms for structural design optimization. J Comput Struct 79:2527–2539

Pourzeynali S, Lavasani HH, Modarayi AH (2007) Active control of high rise building structures using fuzzy logic and genetic algorithms. Eng Struct 29:346–357

Sarma KC, Adeli H (2000) Fuzzy genetic algorithm for optimization of steel structures. J Struct Eng ASCE 126(5):596–604

SEAOC (1995) Performance-Based Seismic Engineering of Buildings, Structural Association of California, Sacramento, CA, USA

Soh CK, Yang J (1996) Fuzzy controlled genetic algorithm search for shape optimization. J Comput Civil Eng ASCE 10(2):143–150

Sung YC, Liu KY, Su CK, Tsai IC, Chang KC (2005) A study on pushover analyses of reinforced concrete columns. J Struct Eng Mech 21(1):35–52

Sung YC, Lin TW, Tsai IC, Chang SY, Lai MC (2007) Application of normalized spectral acceleration-displacement (NSAD) format on performance-based seismic design of bridge structures. J Mech 23(2):86–93

Xue Q, Wu CW (2006) Preliminary detailing for displacement-based seismic design of buildings. J Eng Struct 28(3):431–440

Zadeh LA (1965) Fuzzy sets. J Inf Control 8:338–353

Zou XK, Chan CM (2005) Optimal seismic performance-based design of reinforced concrete buildings using nonlinear pushover analysis. J Eng Struct 27:1289–1302